International Journal of Recent Advances in Multidisciplinary Topics
Volume 7, Issue 2, February 2026
www.ijramt.com | E-ISSN: 2582-7839 | RESAIM Publishing | www.resaim.com

Optimization of a Double Wishbone Torsion Bar Spring Suspension System for a Hub Motor-Driven Vehicle

Zhirui Liu[1], Xiaojun Zou[2], Liukai Yuan[3], Can Cao[3], Rui Lian[3], Liangmo Wang[1*]
[1]*School of Mechanical Engineering, Nanjing University of Science and Technology, Nanjing, China*
[2]*School of Cyber Science and Engineering, Southeast University, Nanjing, China*
[3]*Nanjing Iveco Co., Ltd., Nanjing, China*

***Abstract*: This paper analyzes and optimizes the kinematics of a double-wishbone torsion bar suspension for in-wheel motor EVs, addressing performance degradation due to hard point changes. A parametric model was built in ADAMS/Car. Parallel wheel travel simulation generated curves for toe, camber, caster, and kingpin inclination angles versus wheel travel. Results showed the initial toe angle exceeded its ideal range, and the kingpin inclination failed to stay within the 7~13° design specification, indicating a need for optimization. Using Adams/Insight, sensitivity analysis identified the upper/lower control arm and tie rod inner hard points as critical. DOE and multi-objective optimization were applied to these hard points. Post-optimization results confirm effective improvement: caster angle variation was reduced by 35.9% with a 0.09° downward shift; kingpin inclination variation decreased by 13.6%, its minimum value increased by 0.42°, achieving a more desirable range. This work enhances suspension performance and delivers a systematic optimization method for similar suspension systems.**

***Keywords*: ADAMS/Car, hard point coordinates, independent suspension, multi-objective optimization, positioning parameters.**

1. Introduction

The dynamic variation of wheel alignment parameters during vehicle operation is a critical factor affecting handling stability. As the key component connecting wheels to the body, the suspension system directly determines driving comfort and safety [1],[2]. Research indicates that controlling wheel alignment parameter variations within an optimal range can significantly enhance vehicle stability [3]. Among various suspension configurations, the double wishbone independent suspension is widely adopted due to its superior structural characteristics [4]. The variation patterns of its alignment parameters under bumpy road conditions directly impact steering precision and driving stability.

Electric wheel drive technology is a key technology for electric vehicles. However, due to significant alterations in drive configuration and layout, converting to electric wheel drive causes corresponding changes in vehicle chassis performance [5]. To enhance the dynamic performance of suspension systems, numerous scholars have conducted in depth research: Wang et al. [6] performed an optimization design using ADAMS simulation for a hub motor-driven double wishbone suspension, targeting minimal changes in wheel camber and toe angles to minimize tire wear. Cai et al. [7] investigated the influence of dynamic characteristics on ride smoothness and stability in MacPherson strut suspensions. Yuan et al. [8] optimized the damping and stiffness parameters of an 8×8 wheeled armored vehicle suspension, effectively improving ride comfort. Li et al. [9] utilized Adams/Insight to optimize the steering mechanism of an air suspension, achieving better steady-state response. Chen et al. [10] employed a genetic algorithm to optimize a five-link suspension, setting the minimization of deviation between camber angle changes during wheel bounce and target values as the optimization objective. This approach was applied to an actual passenger car case study. These studies collectively demonstrate that controlling changes in wheel alignment parameters within reasonable limits during vehicle operation is central to enhancing suspension system performance [11]. However, most of the above studies focus on suspensions for conventional drive configurations. When hub motors are installed, their large radial dimensions and mass occupy wheel-side space, significantly altering the distribution of unsprung mass. This causes the original suspension hardpoint layout to fail and degrades the characteristics of the alignment parameters, necessitating methods to restore suspension kinematic performance under strict spatial constraints.

This paper investigates the understeer issues observed during testing of a double wishbone torsion bar spring suspension equipped with a hub motor. A simulation model was established using Adams/Car. Analysis revealed that during wheel vertical movement, the variation range of the kingpin inclination angle exceeded the acceptable limits, constituting the primary cause of diminished handling performance. Consequently, this study further employed the Adams/Insight module to effectively optimize this positioning parameter by adjusting the suspension mounting point location, thereby enhancing suspension performance.

*Corresponding author: liangmo@njust.edu.cn

2. Dual Double Wishbone Suspension Model Establishment

A. Simplification of the Kinematic Model for the Dual Double Wishbone Suspension

For analytical convenience, certain reasonable simplifications are applied when establishing the multi-bar kinematic model of the front suspension. Considering that the purpose of the suspension kinematic analysis is to determine the relationship between various front wheel alignment parameters and wheel vertical movement, the suspension is simplified into a multi-link mechanism. During kinematic analysis, only the positions of several hinge points need to be defined to perform the analysis. The simplified double wishbone suspension model is shown in Figure 1. Here, AE, BE, CF, and DF represent the upper and lower control arms, respectively; EF denotes the kingpin axis of the steering knuckle; GH is the steering knuckle arm; HI is the steering tie rod; and P is the wheel center. The upper and lower control arms connect to the chassis via the pivot joints at points A, B, C, and D, respectively, and link to the upper and lower ball joints of the steering knuckle via the spherical joints at points E and F. The steering knuckle PG connects to the wheel hub via a pivot joint. The steering arm GH is fixed to the steering knuckle. The steering tie rod HI connects to the steering arm via a ball joint at point H. The steering rack connects to the steering tie rod via a universal joint at point I.

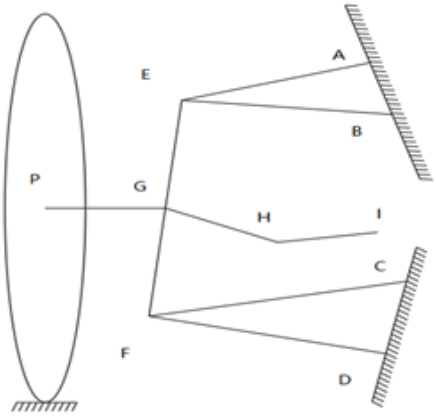

Fig. 1. Topological diagram of double wishbone torsion bar spring suspension structure

B. Development of the ADAMS Model for the Double Wishbone Suspension

The suspension system is symmetrical left and right, with all components assumed to be rigid bodies [12]. Based on the obtained coordinates of suspension-related rigid points, a suspension rigid body model can be established in Adams/Car. Table 1 shows the initial rigid point coordinates for the left side of the double wishbone suspension.

A suspension subsystem comprising components such as the suspension and test platform was further established, resulting in the double wishbone torsion bar spring independent suspension subsystem model shown in Figure 2.

Table 1
Double wishbone suspension hard point parameters

Hard Point	X/mm	Y/mm	Z/mm
bumpstop lower	-20.641	-611.962	233.942
bumpstop upper	-20.641	-599.437	304.977
lca auxiliary arm	-41.098	-581.880	-65.188
lca front	-420.597	-402.397	-60.909
lca outer	-24.550	-782.815	-62.959
lca rear	-21.500	-401.000	-66.412
lwr strut mount	67.726	-585.478	-65.188
reboundstop lower	-20.641	-540.011	118.564
reboundstop upper	-20.641	-564.709	171.529
tbar to body	1161.859	-481.000	198.588
tierod inner	-134.841	-417.494	56.995
tierod knuckle	-18.437	-765.107	83.258
tierod outer	-158.052	-802.945	48.134
top mount	68.129	-540.541	273.584
uca front	-420.590	-483.013	206.476
uca outer	-13.644	-751.224	197.841
uca rear	-20.665	-481.000	198.588
wheel center	-20.701	-1010.538	25.215

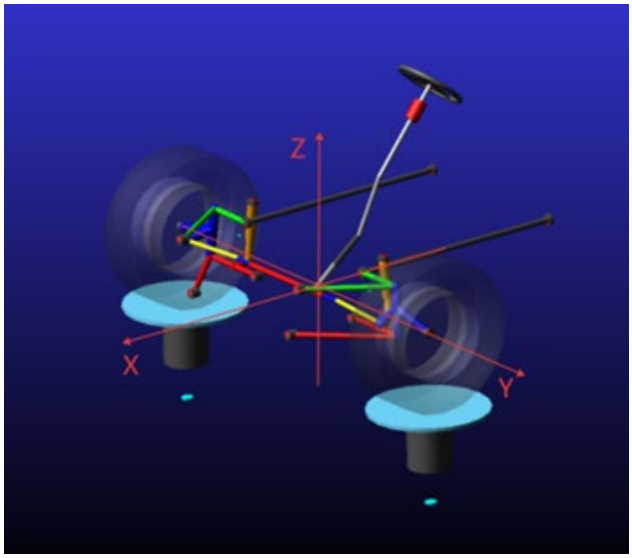

Fig. 2. Subsystem model of the double wishbone suspension

3. Analysis of Suspension Kinematic Characteristics

The kinematic characteristics of a suspension primarily investigate the variation patterns of suspension positioning parameters, which mainly include wheel toe angle, camber angle, caster angle, kingpin inclination angle, and other related parameters. These parameters have a critical impact on vehicle handling stability and driving performance. The parallel wheel bounce test simulates the bumpy motion experienced when a vehicle traverses obstacles or travels on uneven terrain, as well as suspension movement caused by changes in body posture during acceleration and deceleration. [13]. In ADAMS/Car, the wheel bounce range was set to -70 to 70 mm with a simulation step size of 130 steps. Simulating wheel bounce in the same direction allowed investigation of how wheel alignment parameters change. Using ADAMS' post-processing module, response characteristic curves of wheel alignment parameters versus vertical wheel displacement were obtained, as shown in Figure 3 to 6.

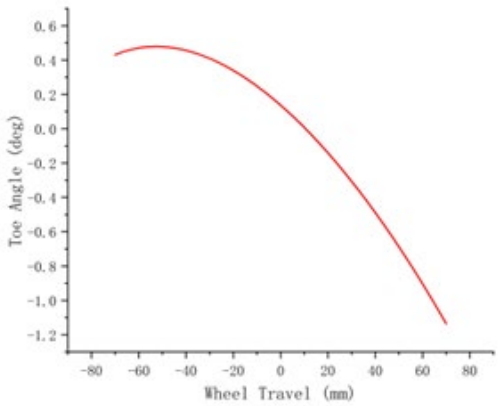

Fig. 3. Initial simulation curve of toe angle

The simulation results were primarily analyzed based on four wheel alignment parameters: toe-in angle, camber angle, caster angle, and kingpin inclination angle. Toe angle counteracts outward rolling tendencies caused by camber, ensuring straight-line stability. As shown in Figure 3, with an initial toe angle of 0.14°, the toe angle varies between 0.43° and 0.48° when the hub vertical displacement ranges from -70 mm to -53.2 mm. When the wheel hub vertical displacement ranges from -53.2 to 70 mm, the toe angle varies between -1.14° and 0.48°, with a change of 1.62°, exceeding the ideal toe angle variation range.

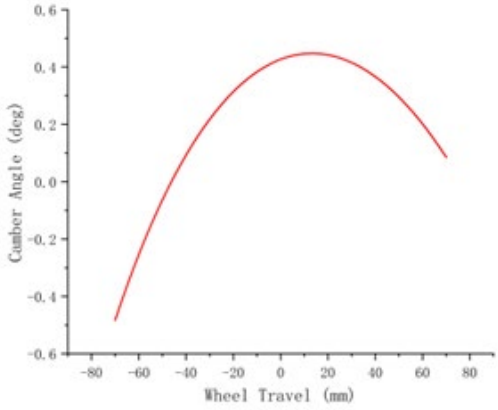

Fig. 4. Initial simulation curve of camber angle

Caster angle ensures maximum tire tread contact with the road surface during vehicle loading and cornering, enhancing handling stability. Therefore, minimal variation in camber angle is required. As shown in Figure 4, with an initial camber angle of 0.43°, when the hub vertical displacement ranges from -70 to -5.6 mm, the camber angle varies between -0.48° and 0.41°; When the hub vertical displacement ranges from -5.6 to 70 mm, the camber angle varies between 0.09 and 0.41°. This 0.89° variation is less than the 1° change range for camber, meeting the ideal variation criteria.

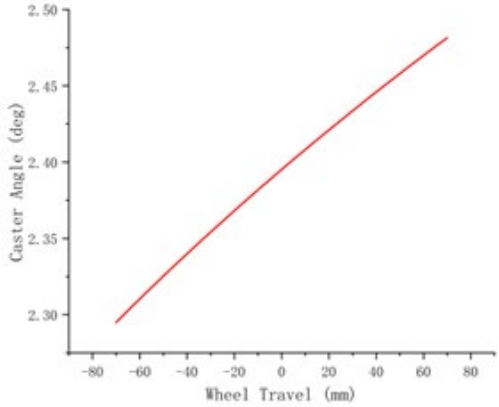

Fig. 5. Initial simulation curve of caster angle

The kingpin inclination generates a steering wheel torque that automatically returns the wheel to center, enhancing high-speed stability. As shown in Figure 5, with hub vertical displacement ranging from -70 to 70 mm, the initial caster angle is 2.40°, with a variation range between 2.30° and 2.58°, meeting the requirement for variation within the 1° to 3° range.

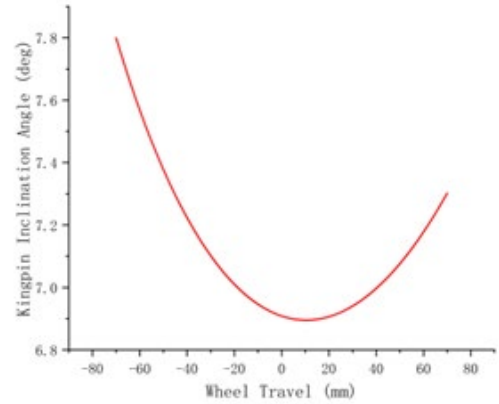

Fig. 6. Initial simulation curve of kingpin inclination angle

Kingpin inclination enables timely automatic wheel return after steering and facilitates light steering effort. During wheel vertical movement, excessive changes in the kingpin inclination angle must be avoided to prevent overly heavy steering and accelerated tire wear. As shown in Figure 6 with an initial kingpin inclination angle of 6.91°, the angle varies between 6.90° and 7.8° when the wheel hub vertical displacement ranges from -70 to 11.2 mm. When the wheel hub vertical displacement ranges from 11.2 to 70 mm, the variation in kingpin inclination angle falls between 6.90° and 7.30°, exceeding the ideal range of 7° to 13°.

The above analysis reveals that the installation of hub motors on the suspension creates unique design conflicts: the dimensions of the hub motors affect the positioning of the wheel-side space, fundamentally compressing and altering the location of suspension hard points and the feasible design domain. This causes the geometry and kinematics of the

kingpin to deviate from the optimal range. Specifically, the toe-in angle and kingpin inclination angle exhibit suboptimal variations with wheel vertical displacement. To address this, a targeted multi-objective optimization method was developed. Its uniqueness lies in prioritizing the constraint of zero spatial interference for the hub motor throughout the full suspension travel range, and more critically, in directly restoring the ideal kinematic curves and suspension-related performance lost due to motor installation.

4. Optimization of Hard Points in Double Wishbone Suspension

A. Selection of Optimization Variables and Objectives

In vehicle design, it is generally desired that the toe-in value remains constant during wheel vertical movement, while the kingpin inclination angle typically requires an ideal variation range of 7–13°. Based on conclusions drawn from simulation analysis, this optimization primarily addresses the undesirable variation patterns of toe angle and kingpin inclination angle. Therefore, this optimization sets the wheel toe value and kingpin inclination angle as the optimization targets. However, optimizing a single wheel alignment parameter can cause opposing trends in other alignment parameters [14]. Thus, when optimizing wheel toe and kingpin inclination angle, other wheel alignment parameters must also be considered. Consequently, simultaneous optimization of multiple objectives—including the variation ranges of four related wheel alignment parameters—is required.

Optimization of double wishbone suspensions typically focuses on two aspects: first, optimizing structural parameters such as upper/lower control arm lengths and tie rod positions; second, optimizing the coordinates of fixed points, which are typically the inner/outer points of upper/lower control arms and the outer point of the tie rod. This paper primarily investigates the influence of the spatial positioning of the double wishbone suspension's steering mechanism on its kinematic performance. Consequently, the optimization focuses on the hard point coordinates of the front and rear points, outer points of the upper and lower control arms, and the inner point of the steering tie rod in the double wishbone front suspension. However, the selected seven rigid points encompass 21 coordinates across three axes (x, y, z). Treating all as optimization variables would require modifying too many parameters, and some rigid point coordinates exert minimal influence on wheel alignment parameters. Therefore, ADAMS/Insight software was first employed to analyze the relationship between these 21 coordinate points and the alignment parameters. Subsequently, sensitivity analysis was applied to comprehensively select optimization variables, identify the degree of influence each hard point coordinate exerts on the suspension's motion characteristics, reduce computational load during optimization, simplify calculations, and shorten the development cycle [15]. Thus, through sensitivity analysis, coordinate points with significant influence on alignment parameters were selected as optimization factors.

B. Suspension Optimization Design

This paper employs the optimal Latin hypercube design, an improved experimental design method that effectively fills the design space and ensures uniform distribution of sampling points within it. This design method exhibits excellent filling and balance properties, making it suitable for various application scenarios. Therefore, after comprehensive consideration, the optimal Latin hypercube is selected for the sampling design in this study, with the minimum number of sampling points n required to satisfy the conditions specified in Equation (1).

$$n \geq \frac{(N+1)(N+2)}{2} \tag{1}$$

In the equation, N represents the number of design variables.

This study has N=21, with a minimum sampling point count n≥231. To ensure sufficient precision, twice this minimum sampling point count is typically used. Additionally, considering the presence of failed experimental designs, the sampling point count can be selected as high as possible. For this study, the sampling point count n=1000 was chosen. After analyzing all coordinate points, the sensitivity analysis results are listed in Table 2.

Table 2
Sensitivity of wheel alignment parameters to hard points

Hard point	Toe/%	Camber/%	Caster/%	Kingpin/%
lca front X	0.14	-1.28	0.33	0.11
lca front Y	7.72	-1.72	-1.26	0.28
lca front Z	14.90	2.26	-27.35	0.03
lca outer X	-5.65	0.25	-16.84	0.04
lca outer Y	5.92	-2.56	0.02	-31.77
lca outer Z	19.75	22.12	5.30	8.62
lca rear X	-0.71	-0.95	0.43	-1.40
lca rear Y	-4.97	4.26	2.42	0.68
lca rear Z	-15.44	-34.10	14.67	-4.12
tierod inner X	2.08	0.27	-0.14	0.05
tierod inner Y	39.05	-1.29	0.05	-0.48
tierod inner Z	-26.78	14.61	9.10	0.34
uca front X	0.15	-0.80	-0.72	-0.27
uca front Y	-0.49	-1.06	2.06	-0.11
uca front Z	23.07	-24.53	29.18	-3.43
uca outer X	-3.03	-0.37	12.91	-0.26
uca outer Y	4.08	11.77	0.24	24.79
uca outer Z	38.05	-27.73	-24.99	-10.42
uca rear X	-4.24	-9.57	-1.73	-1.37
uca rear Y	-3.89	-8.78	-1.59	-1.26
uca rear Z	-13.16	22.23	-21.68	6.49

Through sensitivity analysis, the effect levels of each design parameter on different performance indicators were obtained. However, the sensitivity of these parameters to each indicator is inconsistent. If the sensitivities of these m parameters to the n indicators are ranked sequentially, the result would be an m×n matrix. This matrix does not intuitively reveal the comprehensive contribution of these parameters to all indicators. By employing the TOPSIS comprehensive contribution solution method, this m×n matrix is transformed into a 1×m matrix. This effectively reconciles conflicts among indicators, yielding a comprehensive ranking of structural

parameters. This approach avoids the one-sidedness of single-indicator evaluation, facilitating subsequent selection of optimization objectives.

Based on the results in Table 2, the absolute values of the contribution degrees are taken. Using the TOPSIS comprehensive contribution method, these are converted into an m×n decision matrix. Processing the m×n TOPSIS matrix yields a weighted 1×m decision matrix. This process yields the Si^+ and Si^- values for each evaluation criterion. The Euclidean distances between each factor and Si^+ and Si^- are then calculated, ultimately determining the comprehensive contribution ranking of the front suspension hard point coordinates on performance in Table 3.

Table 3
Comprehensive contribution coefficients for hard point parameters

Hard point	S+	S-	Euclidean distance	Ranking
lca front X	0.27	0.26	0.49	10
lca front Y	0.25	0.27	0.52	6
lca front Z	0.35	0.26	0.42	18
lca outer X	0.35	0.20	0.37	21
lca outer Y	0.28	0.25	0.47	14
lca outer Z	0.16	0.39	0.70	1
lca rear X	0.27	0.26	0.49	12
lca rear Y	0.27	0.27	0.50	8
lca rear Z	0.37	0.25	0.41	20
tierod inner X	0.26	0.26	0.50	7
tierod inner Y	0.20	0.37	0.65	2
tierod inner Z	0.32	0.31	0.49	11
uca front X	0.27	0.25	0.48	13
uca front Y	0.26	0.26	0.50	9
uca front Z	0.23	0.40	0.63	3
uca outer X	0.24	0.30	0.56	5
uca outer Y	0.23	0.32	0.58	4
uca outer Z	0.39	0.30	0.44	15
uca rear X	0.30	0.22	0.42	19
uca rear Y	0.30	0.22	0.43	16
uca rear Z	0.37	0.27	0.42	17

5. Analysis of Suspension Optimization Simulation Results

Six coordinate points with significant influence on alignment parameters were selected for subsequent adjustments, while the remaining points were omitted. The wheel alignment parameters were optimized to obtain the coordinates of the suspension system's hard points after optimization (Table 4).

Table 4
Optimized hard point coordinates

Hard point	Baseline /mm	Optimized /mm
lca outer Z	-62.959	-65.035
tierod inner Y	-417.494	-413.841
uca front Z	206.476	208.212
uca outer Y	-751.224	-750.65
uca outer X	-13.644	-17.201
lca front Y	-402.397	-404.213

Modify the corresponding hard point coordinates on the suspension according to the adjusted hard point coordinates as shown in Table 4. Set the vertical deflection range to -70 to 70 mm. Re-run the adjusted model in Adams/Car for a co-directional wheel hop simulation experiment. The optimized simulation curves for parameters such as toe angle, camber angle, caster angle, and kingpin inclination angle are shown in Figure 7 to 10.

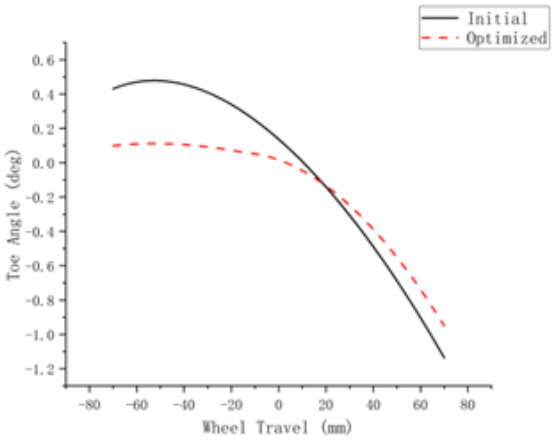

Fig. 7. Toe angle (Optimization comparison)

Figure 7 shows the simulated toe-in angle curve for the wheel. As illustrated, during vertical wheel movement, the variation range of the toe-in angle has been optimized from -1.14° to 0.48° to -0.95° to 0.11°, reducing the variation by 0.56°. This reduction represents 34.6% of the pre-optimization variation range, contributing to enhanced vehicle handling stability. On the other hand, to maintain driving stability and good understeer characteristics, it is generally desirable for the front wheels to exhibit a slight negative toe angle change during upward movement and a slight positive toe angle change during downward movement. The above results indicate that the toe angle optimization has achieved good results.

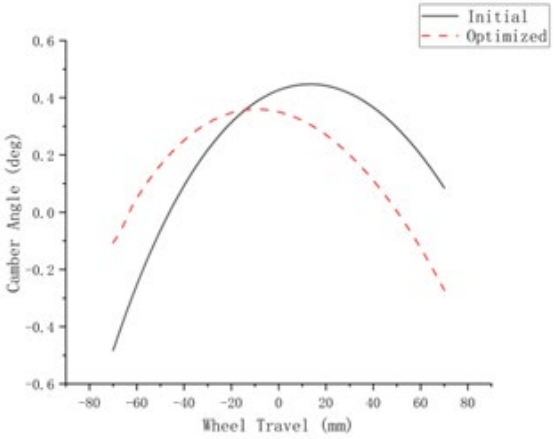

Fig. 8. Camber angle (Optimization comparison)

Figure 8 shows the simulated camber angle curve. The pre-optimization suspension model exhibits camber angle variations ranging from approximately -0.48° to 0.41°, largely meeting the suspension system's design requirements. The optimized camber angle, shown as dashed lines in Figure 8, varies within the range of -0.21° to 0.36°, representing a reduction of 0.32° in variation amplitude. This reduction accounts for 35.9% of the pre-optimization camber variation, This significant narrowing of the variation range reduces tire wear while enhancing ride smoothness and ground stability during routine driving. However, it sacrifices the vehicle's

potential to maintain maximum tire contact patch through negative camber changes during extreme cornering, thereby limiting the handling limits under aggressive driving conditions.

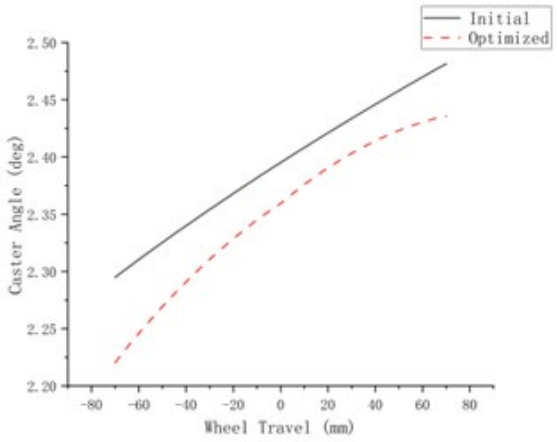

Fig. 9. Caster angle (Optimization comparison)

Figure 9 shows the simulated caster angle curve. The figure indicates that, on one hand, the range before optimization was 2.30–2.48°, while after optimization it became 2.22–2.41°, remaining nearly unchanged. On the other hand, the optimized curve shifts downward by approximately 0.09° overall compared to the pre-optimization curve. This means the optimized caster angle is generally smaller than before. The primary advantage is a significant reduction in steering effort, markedly improving low-speed maneuverability. However, this results in a diminished sense of center and reduced self-centering capability at high speeds, while also causing the steering system's road feedback to become relatively less precise.

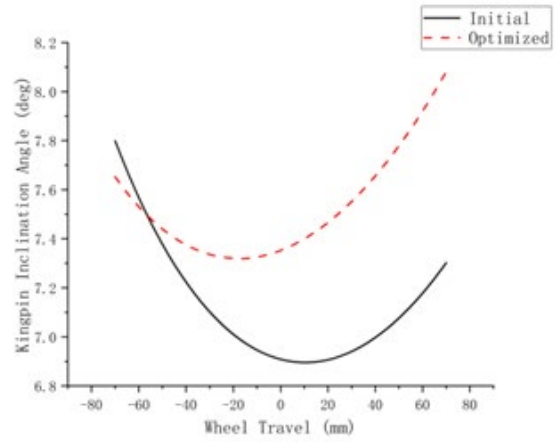

Fig. 10. Kingpin inclination angle (Optimization comparison)

Figure 10 shows the simulated kingpin inclination angle curve. The figure indicates that during wheel vertical movement, the variation range of the kingpin inclination angle shifts from 6.90–7.78° to 7.32–8.08°, reducing the variation by 0.12°. This reduction accounts for approximately 13.6% of the pre-optimization variation range, thereby enhancing suspension handling stability. On the other hand, the optimized curve exhibits a minimum value of 7.32° at -16.6 mm, shifting upward by approximately 0.42°. This ensures the optimized kingpin inclination angle falls within the ideal variation range of 7° to 13°.

Overall, this represents a typical and reasonable optimization strategy that prioritizes everyday comfort, agility, and economy by moderately sacrificing ultimate handling stability and some steering feedback. For the target vehicle, this trade-off generally yields more benefits than drawbacks.

Table 5
Changes in optimized wheel alignment parameters

	Initial /°	Optimized/°	Range/°	Gain/%
Toe	(-1.14,0.48)	(-0.95,0.11)	0.56	34.6
Camber	(-0.48,0.41)	(-0.21,0.36)	0.32	35.9
Caster	(2.30,2.48)	(2.22,2.41)	-0.01	-5.6
Kingpin	(6.90,7.78)	(7.32,8.08)	0.12	13.6

6. Conclusion

This paper employs Adams/Car to establish a simulation model of a double wishbone torsion bar spring suspension for a vehicle equipped with hub motor drive. The model undergoes multi-objective optimization design using Adams/Insight. By optimizing wheel alignment parameters, the vehicle achieves superior driving performance, demonstrating significant engineering design implications.

1) This paper describes the construction of a double wishbone suspension model using Adams/Car software. The addition of hub motors significantly affects the wheelbase and the lateral offset distance at the kingpin. Consequently, the suspension's kinematic characteristics inevitably change, necessitating co-directional bounce simulation experiments.
2) Employing the Adams/Insight optimal Latin hypercube sampling method, the design variables include the positions of suspension hard points (upper/lower control arms), while the design objectives are toe angle, camber angle, caster angle, and kingpin inclination angle. Multi-objective optimization improves suspension performance.
3) Post-optimization results indicate: toe-in variation reduced by 34.6%, camber variation decreased by 35.9%, overall negative caster shift of approximately 0.09°, negative camber variation reduced by about 13.6%, and minimum camber increased by approximately 0.42° to 7.32°, achieving a relatively ideal variation range.

References

[1] W. H. Hu, Y. Shen, and J. Z. Feng, "Simulation analysis of traditional and L type Macpherson suspension based on ADAMS/Car," *Adv. Mater. Res.*, vols. 479–481, pp. 1515–1521, 2012.

[2] C. Kavitha, S. A. Shankar, B. Ashok, *et al*., "Adaptive suspension strategy for a double wishbone suspension through camber and toe optimization," *Eng. Sci. Technol., Int. J.*, pp. 149–158, 2018.

[3] Z. M. Li and J. S. Weng, "Simulation and optimization of locating parameters for independent rear suspension based on ADAMS," *Automotive Applied Technology*, vol. 49, no. 1, pp. 131–135, 2024.
[4] X. Ren, L. Gao, T. Liu, *et al*., "Adams-based performance optimization of mining dump trucks," in *Proc. SPIE*, vol. 12790, p. 8, 2023.
[5] W. Tong and Z. Hou, "Analyses on the vertical characteristics and motor vibration of an electric vehicle with motor-in-wheel drive," *Automotive Engineering*, vol. 36, no. 4, pp. 398–403 and 425, 2014.
[6] D. L. Wang, N. Chen, Y. W. Liu, *et al*., "Design and optimization of in-wheel motor and double-wishbone suspension of electric vehicle," *Machinery Design & Manufacture*, no. 10, pp. 99–103, 2016.
[7] J. Cai and J. Long, "Structural optimization of MacPherson suspension based on Adams and Isight," *IOP Conf. Ser.* (IOP Publishing), 2025.
[8] X. Yuan, "Ride comfort analysis and optimization of 8×8 wheeled armored vehicle based on ADAMS/Car software," in *Proc. SPIE*, vol. 12790, p. 11, 2023.
[9] M. Li, "Using Adams/Car and Insight in simulation and optimization on guiding mechanism of air front-suspension," *Appl. Mech. Mater.*, vols. 635–637, pp. 381–384, 2014.
[10] X. K. Chen and Y. Lin, "Application of genetic algorithm in five-linkage suspension optimization," *Automobile Technology*, no. 12, pp. 5–8, 2004.
[11] L. Wei, J. Li, and J.-Y. Wang, "Modeling and simulation of MacPherson suspension based on ADAMS/CAR," *Machinery*, vol. 39, no. 10, pp. 62–64 and 70, 2012.
[12] J. H. Liang and L. L. Xin, "ADAMS-based double wishbone suspension motion simulation and optimization," *Appl. Mech. Mater.*, vols. 128–129, pp. 34–37, 2012.
[13] J. Zhan, J. Lu, and X. Guan, "Test method of suspension kinematics and compliance," *Appl. Mech. Mater.*, vols. 278–280, pp. 14–17, 2013.
[14] Q.-Q. Xie and C.-G. Fang, "Optimization of double wishbone suspension for electric wheel drive vehicle based on ADAMS/Insight," *Internal Combustion Engine & Parts*, no. 10, pp. 36–38, 2024.
[15] Z. X. Wu, Z. Fu, C. Cheng, *et al*., "Hardpoint position optimization of double wishbone suspension based on kinematic characteristics," *Automobile Technology*, no. 2, pp. 39–43, 2015.